

## Critical plasmons of a Fibonacci semiconductor superlattice: Spectrum and optical properties

Pawel Hawrylak, Gunnar Eliasson, and John J. Quinn

*Department of Physics, Brown University, Providence, Rhode Island 02912*

(Received 22 May 1987)

We study the collective excitations of an array of two-dimensional electron-gas layers arranged in a Fibonacci sequence. The plasmon spectrum is calculated using a transfer-matrix method. It is demonstrated that the spectrum is critical. Global scaling properties of the spectrum are discussed. The infrared resonant absorption and Raman spectra are calculated. They provide information about the structure of frequency spectra and local density of states in reciprocal space.

### I. INTRODUCTION

Electronic and elastic properties of one-dimensional (1D) quasiperiodic systems (IQPS) have been studied extensively.<sup>1</sup> These systems show extended, localized, and critical states associated with metal-insulator transition. This has to be contrasted with disordered systems which show "localization transition" only in higher dimensions. The nature of critical states and the properties of the system at the critical point are of interest. For the system close to the metal-insulator transition, critical states will control properties of the system on a length scale smaller than the correlation length. The remarkable feature of 1D QPS is the existence of a class of entirely critical systems. This has been demonstrated by Kohmoto *et al.*<sup>2</sup> and Ostlund *et al.*,<sup>3</sup> who studied a tight-binding Hamiltonian based on a Fibonacci sequence and found all states to be critical. Recently, Das Sarma *et al.*<sup>4</sup> pointed out that plasmons in modulation-doped semiconductor superlattices exhibit many interesting phenomena, such as localization transition and critical states, in a way similar to electrons. At the same time, charge-density fluctuations can be probed directly by Raman scattering, electron energy loss, and infrared resonant absorption (IRA). We will discuss here a system with an entirely critical plasmon spectrum and how this spectrum can be observed experimentally. Preliminary results have been reported in Ref. 5.

In periodic semiconductor superlattices, such as modulation-doped GaAs-Ga<sub>1-x</sub>Al<sub>x</sub>As, plasmons are now well understood.<sup>6</sup> Plasmons can propagate along the superlattice direction, and the allowed plasmon frequencies form bands characterized by a Bloch index  $k$ . The case of a quasiperiodic superlattice is more challenging because the Bloch theorem is not applicable. Recently, a quasiperiodic semiconductor superlattice has been grown by Merlin *et al.*<sup>7</sup> It consists of two building blocks  $A$  and  $B$  having thicknesses  $a$  and  $b$ , respectively, arranged in the Fibonacci sequence. Each block is composed of GaAs and Ga<sub>1-x</sub>Al<sub>x</sub>As layers. If the Ga<sub>1-x</sub>Al<sub>x</sub>As region is doped with donors, a layer of quasi-two-dimensional electrons can be produced in every block  $A$  and  $B$ . Such a system can be thought of as an array of electron-gas layers, separated by distances

$a$  or  $b$ , arranged in a quasiperiodic (Fibonacci) sequence. Because electrons do not tunnel between the layers, the problem of collective charge-density excitations is essentially that of obtaining a self-consistent solution of the Poisson equation for the induced potential (charge density) on every layer. This problem of solving a quasiperiodic Poisson equation is similar to the problem of solving a quasiperiodic Schrödinger equation, which has been studied in detail.<sup>2,3</sup> It is now well established that the spectrum of a quasiperiodic Schrödinger operator is a Cantor set having pure point components (localized states), components with absolutely continuous measure (extended states), and singular components with critical (self-similar or chaotic) states. We find a similar behavior for the plasmon spectrum. The case of a continuous incommensurate modulation of electron density in equally spaced layers has been studied by Das Sarma *et al.*<sup>4</sup> Using a duality transformation, these authors demonstrated the existence of a "mobility edge" in the plasmon spectrum. For the strength of Coulomb interaction between the layers smaller than a certain critical value, all plasmon states become localized, while for Coulomb interaction above the critical value all plasmon states are extended. Critical states exist precisely at the mobility edge. Any arbitrary small deviation from the critical point, as is bound to happen in experiment, will produce extended or localized states. Our main interest is in critical states, which are the least understood at present. We will show that the system studied here is entirely "critical," i.e., it never admits either extended or localized states, and is therefore ideally suited for the study of critical states.

The rest of the paper is organized as follows. In Sec. II we describe the model and the plasmon spectrum. Global scaling properties are discussed in Sec. III. Section IV contains calculation of the infrared resonant absorption spectrum, and Sec. V deals with plasmon spectrum of finite superlattice and Raman scattering. The discussion and conclusions are in Sec. VI.

### II. THE MODEL AND PLASMON SPECTRUM

Let us consider  $F_m$  two-dimensional electron-gas (2D EG) layers, where  $F_m$  is a Fibonacci number, i.e.,  $F_m$

satisfies a recursion relation  $F_{m+1} = F_m + F_{m-1}$ , with  $F_0 = 1$ ,  $F_1 = 1$ . Let  $l$  label the layers and  $z_l$  be the position of layer  $l$  along the superlattice axis. The distance between layer  $l$  and  $l+1$  is called  $d_l$ , and  $d_l$  can be either  $a$  or  $b$ . The set  $\{d_l\}$  of a's and b's is generated using the Fibonacci rule  $F[a, b] = [ab, a]$ .<sup>3</sup> In practice we start with a single 2D EG layer at  $z_l = 0$ , followed by a semiconductor layer of thickness  $a$ . In the second step, according to the Fibonacci rule, a 2D EG layer followed by a semiconductor layer of thickness  $b$  is added. This gives a string  $\{a, b\}$ . The third generation produces the string  $\{a, b, a\}$  by replacing the element  $a$  with two elements  $a$  and  $b$  and the element  $b$  with the element  $a$  in the string  $\{a, b\}$ . We continue this process  $m$  times. In the  $m$ th generation there are  $F_m$  elements of the string. This includes  $F_{m-1}$  elements  $a$  and  $F_{m-2}$  elements  $b$ . Note that the ratio of the number of elements  $a$  to the number of elements  $b$  approaches the "golden mean" value  $\tau = (1 + \sqrt{5})/2$ .

The potential  $\phi$ , induced on every layer by a perturbation with frequency  $\omega$  and wave vector  $q$  parallel to the layers satisfies the integral equation

$$\phi(l) = \sum_{l'} v_q \Pi(q, \omega) V(l, l') \phi(l'), \quad (1)$$

where  $\phi(l) = \phi(z_l)$ ,  $v_q = 2\pi e^2 / \epsilon q$ ,  $\Pi$  is the polarizability of a 2D electron gas, and  $V(l, l') = \exp(-q |z_l - z_{l'}|)$ . In the long-wavelength limit the product  $v_q \Pi$ , defined as  $X$ , can be written as  $1/\bar{\omega}^2 = (\omega_q/\omega)^2$ , where  $\omega_q^2 = 2\pi e^2 n q / \epsilon m^*$  is the two-dimensional plasma frequency. Here  $n$  is the electron density,  $\epsilon$  is the background dielectric constant, and  $m^*$  is the electron mass. We can rewrite Eq. (1) in the form of the tight-binding Hamiltonian.

$$\bar{\omega}^2 \phi(l) = \sum_{l' (\neq l)} V(l, l') \phi(l') + V(l, l) \phi(l), \quad (2)$$

where  $\bar{\omega}^2$  plays the role of the eigenvalue,  $V(l, l')$  are the hopping matrix elements, and  $V(l, l) = 1$ . The solution to the eigenvalue problem, Eq. (2), gives the plasma modes of the system.

Much of the progress in studying the quasiperiodic Schrödinger operator has been achieved by the transfer-matrix method. Equation (2) cannot be cast in this form due to the long-range hopping matrix elements  $V(l, l')$ , unless only nearest-neighbor hopping is included. Progress is made by another approach.<sup>5</sup> We write the solution to the Poisson equation  $(d^2/dz^2 - q^2)\phi(z) = 0$  in the region between layer  $l$  and  $l+1$  as

$$\phi_l(z) = A_l e^{-q(z-z_l)} + B_l e^{q(z-z_l)}. \quad (3)$$

Standard electromagnetic boundary conditions across the electron layer allow us to connect  $(A_l, B_l)$  with  $(A_{l+1}, B_{l+1})$  via a transfer matrix  $T$ :

$$\begin{pmatrix} A_{l+1} \\ B_{l+1} \end{pmatrix} = T_l \begin{pmatrix} A_l \\ B_l \end{pmatrix}, \quad (4)$$

$$T_l = \begin{pmatrix} (1+X)e^{-qd_l} & X e^{qd_l} \\ -X e^{qd_l} & (1-X)e^{qd_l} \end{pmatrix},$$

where the susceptibility  $X = v_q \Pi$  is the relevant variable. The matrix  $T$  is a  $2 \times 2$  matrix with a unit determinant. Note that  $\{d_l\}$  is a Fibonacci sequence, so the string of matrices  $\{T_l\}$  is also a Fibonacci sequence of matrices  $T_a$  and  $T_b$   $\{\dots T_a T_b T_a T_b T_a T_b T_a\}$  where  $T_a$  ( $T_b$ ) are matrices  $T$  with  $d = a$  ( $b$ ). Equation (4) is conveniently studied by the rational approximation method. A rational approximation  $m$  to a Fibonacci sequence consists of a periodic sequence of unit cells containing  $F_m$  matrices  $T$  obtained in the  $m$ th generation of the Fibonacci sequence. The spectrum consists of  $F_m$  bands and  $F_{m-1}$  gaps. The bands consist of those values of  $X$  for which the trace of the transfer matrix across the unit cell is between  $-2$  and  $+2$ . Following Refs. 2 and 5 we define the matrix  $M_m$  as  $M_m = \prod_{i=1}^{F_m} T_i$ . The matrix  $M_{m+1}$  is a product of two previous Fibonacci products of matrices  $T$ , i.e.,  $M_{m+1} = M_{m-1} M_m$ . By defining  $x_m = \frac{1}{2} \text{Tr}(M_m)$  we obtain a recursion relation for  $x_m$ ,<sup>3,6</sup>

$$x_{m+1} = 2x_m x_{m-1} - x_{m-2}. \quad (5)$$

The starting conditions are  $x_1 = \frac{1}{2} \text{Tr}(T_a) = \cosh(qa) - X \sinh(qa)$ ,  $x_0 = \frac{1}{2} \text{Tr}(T_b) = \cosh(qb) - X \sinh(qb)$ , and  $x_{-1} = \cosh[q(a-b)]$ . The value of  $x_{-1}$  has been deter-

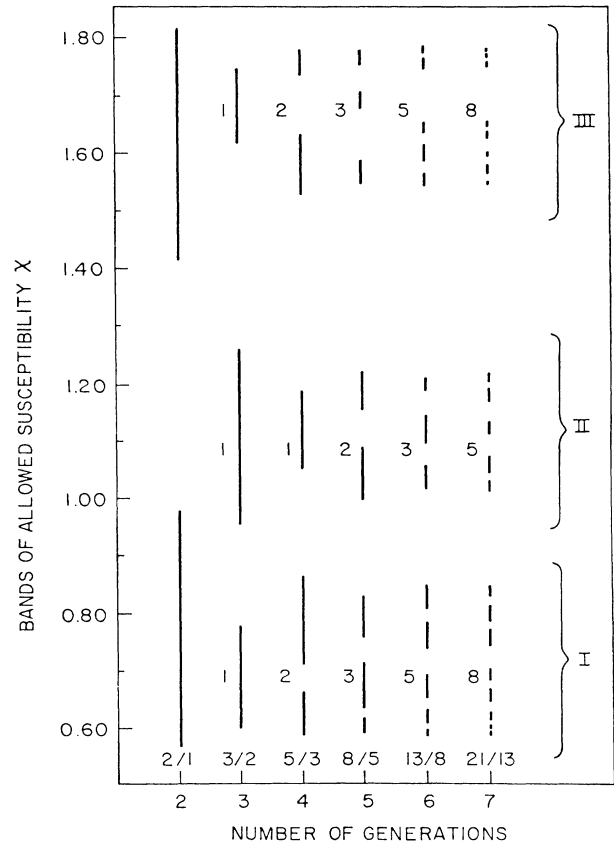


FIG. 1. The allowed values of susceptibility  $X$  for  $qb = 1$ . The band structures for  $m = 2, 3, \dots, 7$  are shown. Note that  $X^{-1} \simeq \omega^2$ . Roman numerals denote three major bands and Arabic numerals enumerate bands for each  $m$ .

mined by requiring that Eq. (5) with  $x_1, x_0$  as defined above, gives  $x_2 = \frac{1}{2} \text{Tr}(T_b T_a)$ . The recursion relation (5) has an important invariant equal to

$$\lambda^2 = -1 + x_m^2 + x_{m-1}^2 + x_{m-2}^2 - 2x_m x_{m-1} x_{m-2}. \quad (6)$$

This quantity remains constant at every step of the recursive formula, Eq. (6). Note that here  $\lambda^2$  is a function of  $X$ . The three-dimensional map given by Eqs. (4) and (5) has been studied by Kohmoto and Oono<sup>2</sup> for the case of  $\lambda^2 = \text{const}$ . Fixed-point analysis yielded escaping, periodic, and chaotic orbits.

We now turn to the plasmon spectrum obtained using Eq. (5). We have set here  $b=1$ ,  $a=\tau$ , and  $q=1$  ( $b$  is the unit of length). In Fig. 1 we plot the bands of  $X$  for various rational approximations  $m$  to the Fibonacci sequence, with  $F_m$  being the size of the unit cell. When  $x_m < 1$ ,  $X$  is allowed, otherwise  $X$  is forbidden. This band structure is very similar to that obtained by Hofstadter,<sup>3</sup> Kohmoto *et al.*,<sup>2</sup> and Ostlund *et al.*<sup>3</sup> As  $m \rightarrow \infty$  we see an infinite number of very narrow bands which have a typical self-similar Cantor set structure. An important quantity here is the total width  $B$  of allowed values of  $X$ . As in Ref. 2, we find that  $B$  scales

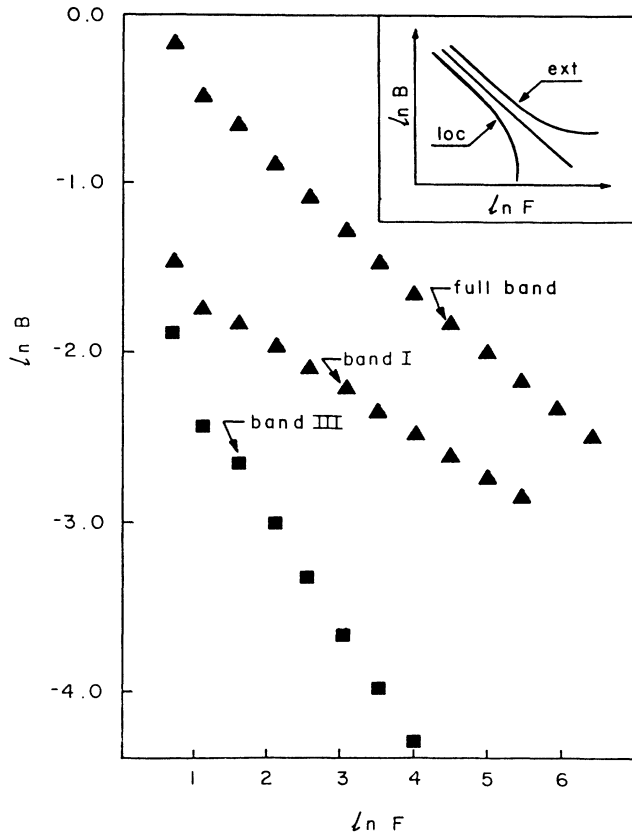


FIG. 2. The dependence of  $\ln B$  on  $\ln F$  for full band and bands I and III.  $B$  is the total bandwidth of the spectrum of Fig. 1. Here  $B$  is the allowed susceptibility values and  $F$  is the size of the unit cell.  $F \rightarrow \infty$  represents quasiperiodic system. The inset shows the typical dependence of  $\ln B$  on  $\ln F$  for localized, extended, and critical states.

with a size of the unit cell as  $B \sim F_m^{-\delta}$ . The scaling index  $\delta$  can be identified as a diffusion constant of the map (Ref. 2). The dependence of  $\ln B$  on  $\ln F_m$  is shown in Fig. 2. This scaling indicates that the spectrum has a zero Lebesgue measure. The inset in Fig. 2 shows schematically the dependence of  $\ln B$  on  $\ln F_m$  for extended, localized, and critical states (Ref. 2). The spectrum of plasmons is clearly critical, with exponent  $\delta$  depending on  $q$ . The measure of the criticality here is more subtle, however. We see that there are two large gaps and three bands. Even though the bands are self-similar, their measure  $B$  scales differently with the number of bands. The dependence of  $\ln B$  for bands I (low  $X$ ) and III (high  $X$ ) on the  $\ln F$  is shown in Fig. 2. Clearly  $B_3$  scales to zero faster than  $B_1$ . In this sense, the low- $X$  (high-frequency) part of the spectrum corresponds to more extended states than the high- $X$  (low-frequency) part of the spectrum. This dependence is due to the dependence of  $\lambda^2$  on  $X$ .

### III. GLOBAL SCALING

Global scaling properties of the plasmon spectrum can be analyzed using the ideas proposed recently for dynamical systems by Halsey *et al.*<sup>8</sup> and applied to a quasiperiodic tight-binding Hamiltonian by Tang and Kohmoto.<sup>2</sup> Let  $\{S_m\}$  be the set of  $F_m$  bands of  $X$ . We define the measure of each band  $i$  in the set of  $\{S_m\}$  as  $P_i = 1/F_m$ . Let the width of the  $i$ th band be  $w_i$ . Then the scaling index  $\alpha$  tells us how the measure scales with the bandwidth, i.e.,  $p_i = (1/F_m) = w_i^\alpha$ . The set of bands with the same scaling exponent  $\alpha$  has a fractal dimension  $f(\alpha)$ , i.e., the number of elements  $N$  in this set is given by  $N(\alpha) = w_i^{-f(\alpha)}$ . The function  $f(\alpha)$  is obtained by introducing a partition function  $\Gamma$  as

$$\Gamma_m(r, s, \{S_m\}) = \sum_{i=1}^{F_m} (F_m)^{-r} w_i^{-s}. \quad (7)$$

The condition

$$\Gamma(r, s) = \lim_{m \rightarrow \infty} \Gamma_m(r, s, \{S_m\}) = 1 \quad (8)$$

uniquely determines the function  $s(r)$ . Then the scaling indices  $\alpha$  and the function  $f(\alpha)$  are given by

$$\begin{aligned} \alpha(r) &= \frac{ds}{dr}, \\ f(r) &= r\alpha(r) - s(r). \end{aligned} \quad (9)$$

The function  $f(\alpha)$  for the plasmon spectrum, i.e., the fractal dimension of the set of bands of  $X$  scaling with the same scaling index  $\alpha$  is shown in Fig. 3 for  $qb=1.0$  and for the finite number of bands  $F_{15}=987$ . There is a finite interval of the scaling indices  $\alpha$ ,  $0.459 < \alpha < 0.861$ . The most probably scaling exponent  $\alpha=0.745$  corresponds to the maximum of  $f(\alpha)=0.709$ , which is the Hausdorff dimension of the set. Our results for the plasmon spectrum are similar to those of Tang *et al.*<sup>2</sup> for the quasiperiodic tight-binding Hamiltonian.

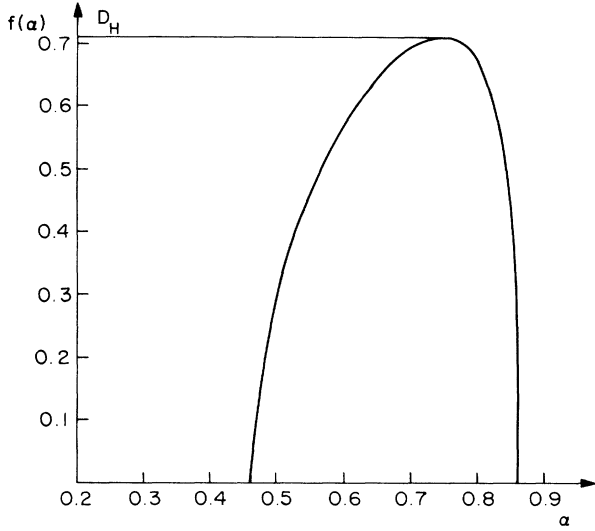


FIG. 3. The function  $f(\alpha)$  for the plasmon spectrum shown in Fig. 1(a). Here  $f$  is a fractal dimension of a set of bands scaling with the scaling index  $\alpha$ .

#### IV. INFRARED RESONANT ABSORPTION

We now turn to experimental techniques which would allow for the direct observation of plasmon spectra of Fig. 1. Since we are interested in the structure of frequency spectra, Raman scattering (discussed in Sec. V), which couples to plasmons with a well-defined wave vector along the superlattice axis, is not very useful. The appropriate technique is infrared absorption of electromagnetic waves in superlattices, achieved by a grating coupler on the surface of the superlattice. The electric field of the wave passing through the diffraction grating can be represented by a Fourier series in  $\cos(q_s x)$ , where  $q_s = 2\pi s/L$ ,  $L$  is the period of the diffraction grating and  $s = 0, 1, 2, \dots$ . The harmonics with  $s > 1$  correspond to the electric field which attenuates exponentially with increasing distance from the diffraction-grating plane. These evanescent waves interact resonantly with plasma oscillations of the superlattice if the frequency of the incident radiation is in the plasmon band. The theory of resonant infrared absorption in periodic superlattices has also been formulated by Krasheninnikov and Chaplik.<sup>9</sup> The total work  $Q$  performed by an external field  $E_{0,x} e^{iqx - qz} e^{-i\omega t}$  parallel to the layers is

$$Q = \frac{1}{2} \text{Re} \sum_l E_{0,x}^* (l) j_x(l), \quad (10)$$

where  $j_x(l)$  is the current on layer  $l$  in the direction  $x$  of applied field. The current is related to the total electric field component  $j_l(x) = \sigma_{xx} E_{\text{tot},x}(l)$  where we take  $\sigma_{xx} = ine^2/m\omega$ . We can express the electric field components in terms of the total and external potential, e.g.,  $E_{0,x}(l) = -iq\phi_0(l)$ , and arrive at the expression for absorbed power  $Q$ :

$$Q(4\pi b/\epsilon |\phi_0|^2 \omega_q) = -\text{Im} \left[ \left\{ \omega/\omega_q \right\} qbX \sum_l \phi_{\text{tot}}(l) e^{-qz_l} \right]. \quad (11)$$

Here  $\phi_{\text{tot}}(l)$  is the total potential on layer  $l$ , measured in units of external potential on first layer  $\phi_0(0)$ . For a periodic, semi-infinite system with a unit cell obtained in the  $m$ th generation of a Fibonacci sequence, the total potential in the superlattice can be written in terms of the coefficients  $A_l, B_l$  and the transfer matrix  $T_l$  as given by Eqs. (3) and (4). Let  $M$  be the transfer matrix across the unit cell with  $F$  layers, i.e.,  $M = \prod_{l=0}^{F-1} T_l$  of length  $d$ . We introduce the ansatz

$$\begin{pmatrix} A_F \\ B_F \end{pmatrix} = M \begin{pmatrix} A_0 \\ B_0 \end{pmatrix} = e^{-ikd} \begin{pmatrix} A_0 \\ B_0 \end{pmatrix}. \quad (12)$$

Equation (12) has nontrivial solutions when  $\cos(kd) = \frac{1}{2} \text{Tr}(M)$ , which determines  $k$ , and moreover in this case  $A_0 = \alpha B_0$  and  $\alpha = M_{12}/(e^{-ikd} - M_{11})$ .

In addition, we must match the total electric fields across the first layers of the superlattice. Noting that the external field has a component only in the layer plane but the total field does not, we find that

$$\begin{aligned} A_0 &= \phi_0 / \{2[\alpha(1-x) - x]\}, \\ B_0 &= \phi_0 \alpha / \{2[\alpha(1-x) - x]\}. \end{aligned} \quad (13)$$

The total potential on every layer is now simply generated using transfer matrices and absorbed power calculated using Eqs. (11) and (12). The results are well illustrated in the case of a system with one layer per unit cell ( $F_1 = 1$ ). In this case we have the total potential on layer  $l$  and absorbed power

$$\phi_{\text{tot}}(l) = \frac{\sinh(qd)}{e^{ikd} - e^{-qd}} e^{-ikld}, \quad (14)$$

$$\cos(kd) = \cosh(qd) - X \sinh(qd),$$

$$Q / \left[ \frac{\epsilon |\phi_0|^2 |\omega_q}{4\pi b} \right] = \frac{1}{2} (\omega/\omega_a)^3 qb e^{qb} \sin(kd). \quad (15)$$

Note that the external potential is a decaying wave, but for the frequency and wave vector in a plasmon band the total potential is a propagating wave, i.e.,  $|\phi(l)|^2 = \text{const}$  on every layer. Our results are in agreement with Krasheninnikov and Chaplik, who used the Wiener-Hopf method. Our method can, however, be very easily extended to systems with large unit cells, which are of interest here.

The absorption bands for  $F_1 = 1$ ,  $F_6 = 13$ , and  $F_9 = 55$  layers per unit cell are shown in Fig. 4, where the value of  $qb = 0.1$  has been chosen, which can be achieved experimentally. Absorption occurs in the frequency interval corresponding to the plasmon band. As the number of bands increases, the power spectrum becomes more and more fragmented as the bands begin to form a Cantor set. Clearly, high-frequency bands give higher absorption than the low-frequency bands. Note also what seems to be a set of divergencies or spikes in some of the bands. These are actually smooth shoulders but we have no physical explanation for their origin. In experiments all sharp features would be rounded off by a broadening due to the finite electronic mobility.

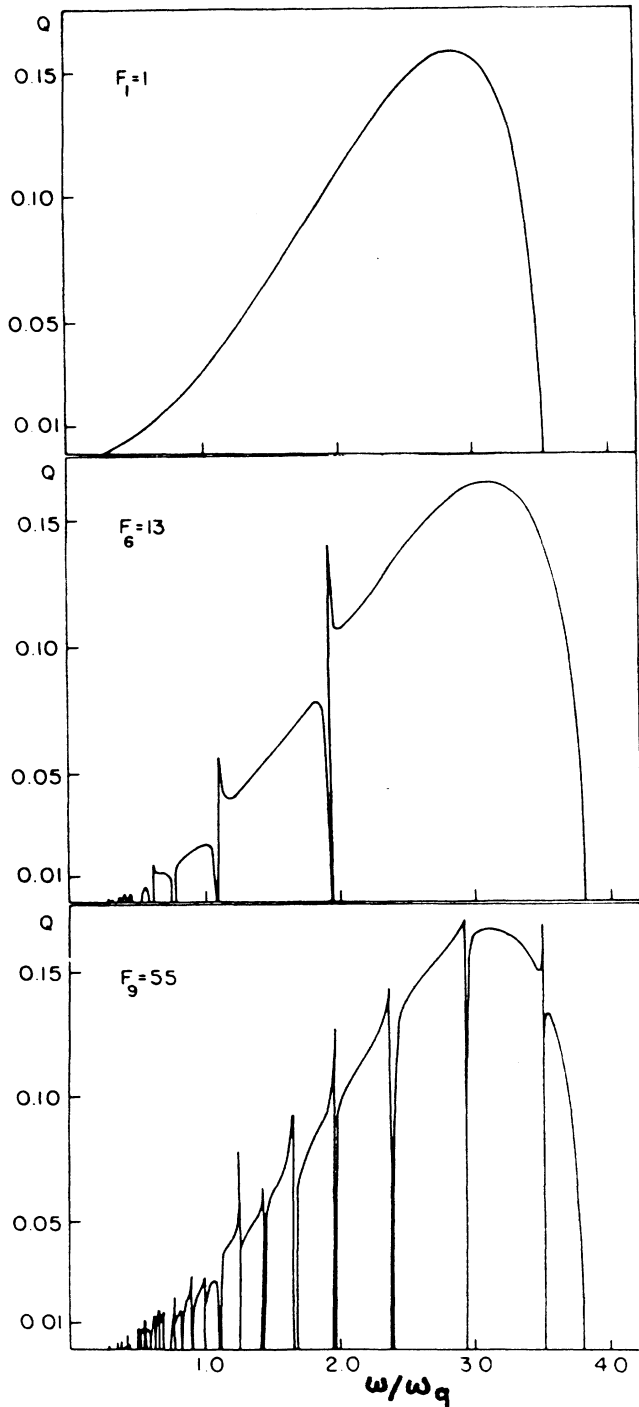


FIG. 4. The evolution of the plasmon infrared absorption spectrum  $Q(\omega)$  with the Fibonacci generation number  $m$ . The cases with  $m=1$ ,  $m=6$ , and  $m=9$  are shown. Here  $F_m$  denotes the number of layers in a unit cell and  $qb=0.1$ .

### V. FINITE SYSTEMS AND RAMAN SCATTERING

We have analyzed a Fibonacci superlattice using a rational-approximation scheme with periodic boundary conditions, i.e., for an infinite system. For finite systems

the methods developed here can also be used. Instead of plasmon bands we then find discrete plasmon modes. The frequency distribution of these modes closely follows the frequency distribution of plasmon bands, as in Fig. 1.

The plasmon frequencies and the induced potential can be calculated either by solving Eq. (1) or using the transfer-matrix method. The boundary conditions in the last case require the induced potential to decay away from the superlattice. Plasmon modes are obtained from the zeros of the determinant of a total transfer matrix  $M$ , while induced potentials are then simply generated for each plasmon frequency by applying transfer matrices to coefficients  $(A_0, B_0)$  on the first layer. The plasmon frequency spectrum resembles the spectrum obtained by the rational approximation method and shown in Fig. 1, if we identify plasmon bands with plasmon modes. For the illustration of eigenvalues and eigenvectors we have chosen the highest eigenvalue  $X_0$  in the central band. This eigenvalue can be characterized by a generalized Bloch index  $K(X)$  where  $K(X)$  is defined as<sup>1</sup>

$$K_n(X) = \int_{-\infty}^X dX' \rho_n(X'), \quad (16)$$

with  $\rho_n(X')$  being the density of plasmon modes for a system of  $F_n$  blocks. In our case  $K_n(X_0) = (F_n - 1)/F_n$  and it is well defined as  $n \rightarrow \infty$ :  $K_n(X_0) \rightarrow 1/\tau$ . If one was to plot  $K_n(X)$ , gaps would be seen at any scale of  $X$ . This is the manifestation of the fact that the set of gaps is dense, or equivalently, that the spectrum has a zero Lebesgue measure. In Fig. 5 we show eigenvalues for four different system sizes ( $F_9, F_{10}, F_{11}, F_{12}$ ). Note the oscillatory character of the Bloch index and eigenvectors with period two. These eigenvectors correspond to a two-cycle of a Fibonacci sequence. The fractal, highly discontinuous structure of induced potential is apparent.

We now turn to Raman scattering. For the energy loss  $\omega$  and momentum transfer  $(q, k)$  from the photon to the plasmon in the backscattering geometry, Raman intensity is given by<sup>10</sup>

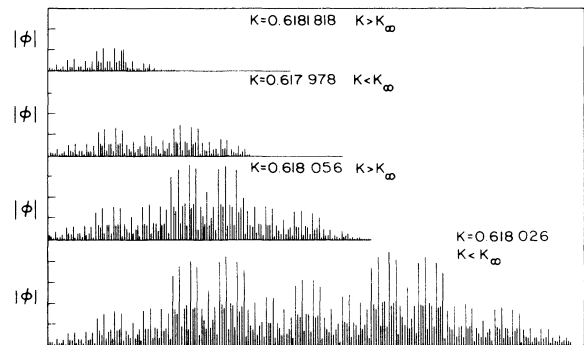


FIG. 5. Absolute value of the induced potential as a function of position for different system sizes for two-cycle of a Fibonacci sequence. Each eigenvalue is characterized by a generalized Bloch index. Note both the oscillatory character of the Bloch index and the structure of the induced potential.

$$I(\omega, q, k) = -\text{Im} \left[ \sum_{l, l'} \tilde{\Pi}(q, \omega, l, l') e^{ik(z_l - z_{l'})} \right], \quad (17)$$

where the polarizability matrix  $\tilde{\Pi}(q, \omega, l, l')$  satisfies the matrix equation

$$\tilde{\Pi}(l, l') = \Pi \delta_{l, l'} + v_q \Pi \sum_{l''} V(l, l'') \tilde{\Pi}(l'', l'). \quad (18)$$

Using the fact that  $v_q \Pi = X = \bar{\omega}^{-2}$  we can write

$$\tilde{\Pi}(l, l') = (\bar{\omega}^2 - V)_{l, l'}^{-1} \bar{\omega}^2 \Pi. \quad (19)$$

The induced potential satisfies Eq. (2)

$$\bar{\omega}_m^2 \phi_m(l) = \sum_{l'} V(l, l') \phi_m(l'), \quad (20)$$

with  $\bar{\omega}_m^2$  being the square of plasmon frequencies. Using the identity

$$(\bar{\omega}^2 - V)_{l, l'}^{-1} = \sum_m \phi_m(l) \frac{1}{\bar{\omega}^2 - \bar{\omega}_m^2} \phi_m^*(l'), \quad (21)$$

one finds that

$$I(\omega, q, k) \approx \sum_m |\phi_m(k)|^2 \delta(\bar{\omega}^2 - \bar{\omega}_m^2), \quad (22)$$

where  $\phi_m(k) = \sum_l e^{ikz_l} \phi_m(l)$  is the Fourier transform of the induced potential. Hence, as pointed out in Ref. 2, the Raman intensity measures the plasmon density of states in reciprocal space.

It is worthwhile to remark that the power  $Q$  can also be written in a similar way:

$$Q(\omega, q) \approx \sum_m |\phi_m(q)|^2 \delta(\bar{\omega}^2 - \bar{\omega}_m^2), \quad (23)$$

where  $\phi_m(q) = \sum_l e^{-qz_l} \phi_m(l)$ . Obviously the main contribution to  $Q$  comes from the states which have a significant amplitude in the vicinity of the superlattice surface.

We now turn to Raman intensities. Two Raman spectra are shown in Fig. 6 for a finite set of  $n = 34$  layers. Figure 6(b) shows a Fibonacci spectrum, while Fig. 6(a) shows a periodic approximation  $\{aba\}$ . The intensity in both spectra is normalized to the highest peak and the integrated intensities are identical. The spectrum for a periodic system shows two sharp peaks, broadened due to finite-size effects (the third peak has intensity too low to be visible). The spectrum for a Fibonacci sequence consists of two broad but well-resolved peaks and some background, and is intermediate to that of a periodic and disordered system. The positions of the peaks in Figs. 6(a) and 6(b) do not correspond to each other. Both spectra are easily distinguishable and Raman scattering should prove useful in studying *critical* plasmons.

## VI. SUMMARY

We have studied plasmons in arrays of two-dimensional layers arranged in a Fibonacci sequence. To obtain the plasmon spectrum, a transfer-matrix technique has been used. This allows for drawing analogies with previously studied electronic, phonon, and dynamical systems. It has been demonstrated that the plasmon spectrum is critical. Global scaling properties of the spectrum have been analyzed. Special emphasis has been placed on experimental techniques, i.e., infrared resonant absorption and Raman scattering. The theory of IRA and Raman scattering based on transfer matrices has been formulated and both spectra calculated. The IRA is suitable for measuring global structure of the spectrum, while Raman spectra provide information about local density of states in reciprocal space. Both techniques should be useful in unraveling the intriguing properties of critical plasmon states.

## ACKNOWLEDGMENTS

The authors acknowledge financial support by the U. S. Army Research Office, Durham, NC. The work of one of us (G.E.) was supported by IBM, and we would like to thank Professor A. Houghton for many stimulating discussions.

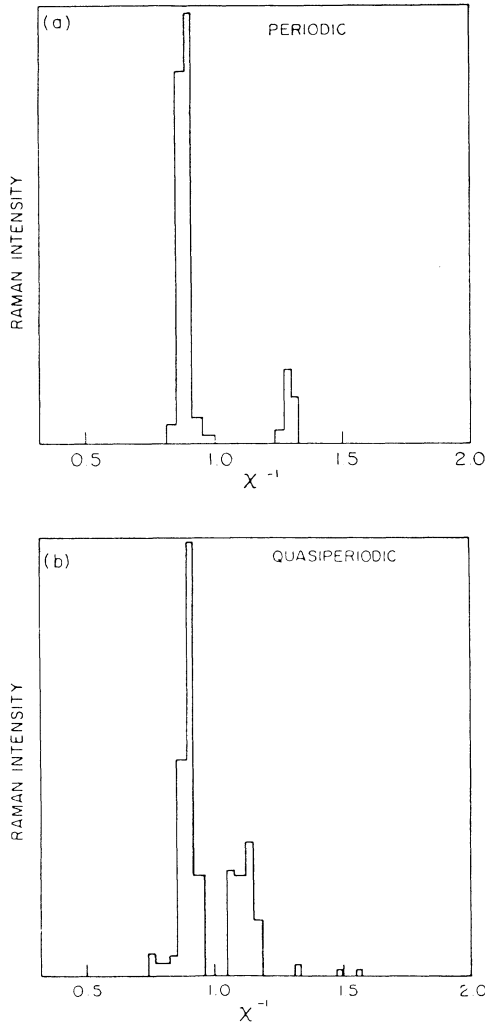


FIG. 6. Raman intensities for a finite system of  $m = 34$  electron layers: (a) periodic and (b) quasiperiodic, as a function of  $X^{-1} = \bar{\omega}^2$ . Parameters are  $qb = 1$ ,  $kb = 1$ .

- <sup>1</sup>For a review, see B. Simon, *Adv. Appl. Math* **3**, 463 (1982); and J. B. Sokoloff, *Phys. Rep.* **126**, 189 (1985).
- <sup>2</sup>M. Kohmoto, L. P. Kadanoff, and C. Tang, *Phys. Rev. Lett.* **50**, 1870 (1983); M. Kohmoto, *ibid.* **51**, 1198 (1983); M. Kohmoto and Y. Oono, *Phys. Lett.* **102A**, 145 (1984); C. Tang and M. Kohmoto, *Phys. Rev. B* **34**, 204 (1986).
- <sup>3</sup>S. Ostlund, R. Pandit, D. Rand, H. J. Schellnhuber, and E. D. Siggia, *Phys. Rev. Lett.* **50**, 1873 (1983); S. Ostlund and R. Pandit, *Phys. Rev. B* **29**, 1394 (1984); D. R. Hofstadter, *ibid.* **14**, 2239 (1976).
- <sup>4</sup>S. Das Sarma, A. Kobayashi, and R. E. Prange, *Phys. Rev. Lett.* **56**, 1280 (1986).
- <sup>5</sup>P. Hawrylak and J. J. Quinn, *Phys. Rev. Lett.* **57**, 380 (1986).
- <sup>6</sup>A. C. Tselis and J. J. Quinn, *Phys. Rev. B* **29**, 3318 (1984).
- <sup>7</sup>R. Merlin, K. Bajema, R. Clarke, F.-Y. Juang, and P. K. Bhatnagar, *Phys. Rev. Lett.* **55**, 1768 (1985).
- <sup>8</sup>T. C. Halsey, M. Jensen, L. P. Kadanoff, I. Procaccia, and B. Schraiman, *Phys. Rev. B* **33**, 1141 (1986).
- <sup>9</sup>M. V. Krasheninnikov and A. V. Chaplik, *Zh. Eksp. Teor. Fiz.* **84**, 1075 (1983) [*Sov. Phys.—JETP* **57**, 624 (1983)].
- <sup>10</sup>J. K. Jain and P. B. Allen, *Phys. Rev. Lett.* **54**, 2437 (1986).